Fuel 153 (2015) 110–117

Contents lists available at ScienceDirect

Fuel

journal homepage: www.elsevier.com/locate/fuel

Porosity evolution in oil-prone source rocks

Saeed Zargari [a], Karen Lyn Canter [b], Manika Prasad [a,*]

[a] Colorado School of Mines, 1600 Arapahoe St., Golden, CO 80401, USA
[b] Whiting Petroleum Corporation, 1700 Broadway, Suite 2300, Denver, CO 80290, USA

HIGHLIGHTS

- Organic rich shales contain considerable amount of porosity in the oil window.
- Extracting the entrapped bitumen allows us to effectively access and measure porosity.
- Kerogen porosity is the dominant pore morphology in organic rich shales (ORS).
- Specific surface area and porosity are directly related to TOC in ORSs.

ARTICLE INFO

Article history:
Received 20 December 2014
Received in revised form 18 February 2015
Accepted 18 February 2015
Available online 28 February 2015

Keywords:
Organic rich shales
Kerogen
Bitumen
Thermal maturity
Porosity

ABSTRACT

The origin of porosity and mechanisms of fluid flow in the presence of organic matter and clay minerals in source rocks are poorly understood. Burial and maturation of the source rock modify or create the pore systems in these rocks. Kerogen decomposition and consequent shrinkage may change the load bearing state of the minerals and organic matter and affect pore system since early stages of maturation. Geochemical evidence confirms that the hydrocarbon expulsion process (i.e. primary migration) is not 100% efficient. Expulsion of hydrocarbon is mainly driven by (1) pressure increase in the source rock due to solid kerogen conversion and volume increase and (2) continued compaction of the sediment. Converted organic matter is partly retained in the source rock diverse framework constituents. Quantitative measurement of and determining producibility of the retained hydrocarbon in the source rock is to date highly debated. The source rock hydrocarbon storage capacity is controlled by pore-hosting particles, pore system topology and rock–fluid interactions.

The presence of organic matter and clay minerals affect log responses by generally overestimating porosity, because the low density kerogen is not accounted for, and together with low resistivity caused by presence of clay minerals can result in erroneous saturation calculations; thus, accurate reserve estimation often is challenged if the impact of low organic matter density is not explicitly addressed.

In order to understand porosity evolution and the interaction of organic byproducts (i.e. bitumen and pyrobitumen) with rock minerals during thermal maturation, one must study source rock samples with different maturities. For this reason, ten Bakken Shale samples with varying maturity and mineralogy were selected in this study. Pore size distributions (PSD), specific surface areas (SSA) and geochemical characteristics of the samples were measured in native state and after successive solvent extraction.

The PSD and SSA measured after each extraction shows recovery of the pore system with successive cleaning. Most significant was the recovery of kerogen-hosted pores with removal of soluble, oil-like organic material. Using successive extractions we are able to determine the evolution of organic matter porosity through maturation which is otherwise not feasible using visual techniques or other conventional laboratory procedures.

1. Introduction

Pore size distribution (PSD), tortuosity, pore aspect ratio, and surface properties are the main pore characteristics which are defined by rock composition, fabric and its burial and diagenetic history. These aspects influence the petrophysical characteristics

Abbreviations: TOC, total organic carbon; SEM, scanning electron microscopy; HI, hydrogen index; SSA, specific surface area; PSD, pore-size distribution; BET, Brunauer–Emmett–Teller (BET) theory.

* Corresponding author. Tel.: +1 303 273 3457.
E-mail addresses: szargari@mines.edu (S. Zargari), lyn.canter@whiting.com (K.L. Canter), mprasad@mines.edu (M. Prasad).

http://dx.doi.org/10.1016/j.fuel.2015.02.072
0016-2361/

of the rock as well as our measurement of these properties. Accessibility of the pore system by the displacement fluid, wettability and surface properties of the grains are the main controls on acquiring reliable and consistent laboratory measurements.

In low porosity rocks with permeability in the nanoDarcy range, porosity measurement comes with unique challenges, e.g., due to, but not limited to, nanometer-sized pores and reactive clay minerals. Conventional methods to measuring porosity and PSD in fine grained, ultra-tight rocks usually yield inconsistent values [1–3]. Defining effective porosity in ultra-tight self-sourcing reservoirs with clay minerals and/or organic matter presents yet another challenge. Clay porosity in conventional reservoirs is considered as an ineffective pore system in storage and flow. Recent studies have questioned this assumption and shown that at certain circumstances, the clay minerals could improve storage and/or flow of hydrocarbons in ultra-tight rocks [4].

Log-derived porosity is calculated from density, neutron and/or sonic logs. These calculations require knowledge of density, hydrogen index and mechanical properties of rock fragments. Kerogen has lower density, lower elastic modulus, higher Poisson's ratio and higher hydrogen content than inorganic minerals [5–8]. Scarcity of accurate measurements of kerogen properties and high contrast between physical properties of kerogen and inorganic minerals makes conventional log interpretation techniques difficult to apply to organic rich rocks.

Pore systems in organic rich rocks matrix can be divided into three pore types as defined by Loucks et al. [9]. Two types of pores are associated with the inorganic minerals (as interparticle and intraparticle mineral porosity) and the third type is associated with the organic matter (intraparticle organic porosity). All types of pores evolve since the time of deposition due to burial, diagenesis and maturation. Clay minerals also undergo significant porosity reduction due to compaction [10].

Porosity in kerogen may exist in the original particle at the time of deposition (e.g., original cellular microstructure in plant material or recycled thermally mature vitrinite), but more commonly, in Type II organic matter it is generated during burial, with early stages of porosity development due to decomposition and catagenesis. Kerogen porosity (if preserved) is often filled with bitumen at early stages of maturation [11,7]. Confirming existence of intraparticle kerogen porosity using SEM image analysis techniques, based on material density contrast, is very challenging since the density of kerogen and bitumen are close. Kuila et al. [12] studied nano-scale pore structure of source rocks by comparing the PSD before and after removal of organic matter by NaOCl treatment. They found significant reduction in abundance of nanometer-size pores after removal of organic matter in mature source rocks indicating storage space within the kerogen. Prasad et al. [6] have shown that with increasing maturity, kerogen particles are sheltered in a supporting frame of stiffer minerals. It is speculated that intraparticle organic porosity in kerogen is well preserved if the kerogen particles are sheltered by load bearing stiff minerals [13]. Determining the fraction of organic matter that is sheltered by such framework of stiff detrital or diagenetic minerals is therefore essential.

The interaction between organic matter maturity and minerals changes effective porosity and other geophysical properties of the mudrocks [14]. Sorption and absorption of hydrocarbon in the organic matter and on the surface of clay minerals also affect the hydrocarbon storage capacity and fluid flow [15–18]. Bitumen and other byproducts of kerogen maturation occupy clay and kerogen porosity in the early stages of oil generation [7,12]. Different mechanisms through which clay minerals and organic matter may interact are widely studied [19–23]. The interaction of clay minerals and organic compounds is mainly governed by the electrically charged surface of the clay minerals and the polar nature of some functional groups present in the bitumen [20]. Based on tendency of some organic functional groups to be adsorbed at clay exchange sites [19–23], it is possible that some organic compounds form stronger bonds with external clay surfaces, replacing clay bound water and consequently dehydrating the source rock. This phenomenon may cause a dramatic increase in resistivity by eliminating the water from interparticle clay porosity and occupying cation exchange cites of the clays.

Previous studies on characteristics of the pore system in source rocks provide limited information about how their pore systems evolve. These studies are mostly focused on investigating the pore system in samples as received with limited pre-treatments or with limited discussion on how pretreatments affect measurements of porosity and PSD [9,12,13,24–26]. We previously observed that considerable amount of bitumen is generated and stored in the source rocks in the oil window [7].

Lack or presence of bitumen in the pore system may introduce significant discrepancy in our evaluation of porosity and pore characteristics [27–30]. However, there are no sharp boundaries between bitumen and hydrocarbons; converted kerogen (hydrocarbons or bitumen) are by definition soluble in organic solvents. If anything, it is the converted organic matter that can contribute to production from source rocks. Therefore, determining the amount of storage specified to the soluble hydrocarbons provides an estimate of effective porosity in organic rich shales. In this study, solvent extraction was performed to determine what portion of the total pore space is excluded from quantification due to oil trapped in pores and to understand the storage and flow capacity of source rocks in the oil window.

2. Material and methods

2.1. Visual techniques

One of the most debated topics related to pore systems in organic rich shales at the oil window is the contribution of each pore hosting grain in total voidage and accessibility and contribution of different pore types in hydrocarbon storage and ultimately, production. Mineralogy, organic richness and thermal maturity determine the types of pores, interaction between generated hydrocarbons and minerals, and control changes in pore-hosting particles.

Visualization techniques have been widely used for petrographical analysis. SEM imaging and thin section analyses are used to understand pore structure, pore morphology and effect of compaction and diagenesis on pore systems. Due to fine-grained nature of mudrocks and complex sub-micron sized pores, 2-D and 3-D SEM imaging techniques have received broad attention for studying porosity and pore structure of mudrocks [9,31–35]. High resolution imaging and image processing techniques have led to development of a new branch of rock physics, the so-called "Digital Rock Physics". However, since digital rock physics is dependent on high resolution images, it is biased toward visible porosity. A considerable portion of the pore system may remain saturated with bitumen and will be counted as a part of solid organic matter due to low optical and density contrast with the kerogen.

This study is focused on quantifying porosity in organic rich rocks at different maturities with emphasis on bitumen-filled porosity in the oil window. This porosity quantification can help understand evolution of porosity and porosity topology in organic rich shales as well as improve digital rock models.

In the following section, we discuss petrographic results of three Bakken Shale samples at immature, mature (oil window) and overmature (gas window) states to visually and quantitatively examine porosity evolution with increasing thermal maturity.

2.2. Porosimetry

Conventional direct porosity measurement techniques often result in inconsistent and inaccurate results when performed on very tight mudrocks [36]. These methods include helium porosimetry, mercury injection porosimetry (MICP) and immersion techniques. Low permeability, small grain and pore sizes, and complex surface properties limit accessibility to mudrock pore system. Luffel and Guidry [37] suggested using crushed tight rock samples for porosimetry purposes to increase material surface area. This technique was later adopted by Gas Research Institute (GRI). The GRI technique includes measuring bulk volume using immersion technique, then crushing and cleaning the sample using Dean Stark solvent extraction. Ultimately the sample is dried and the pore volume is measured with helium pycnometry.

Kuila et al. [38] proposed water immersion porosity (WIP) technique for total porosity measurement in mudrocks. This technique, tested on several nano-Darcy permeability samples, produced more repeatable and reliable results than other methods. Since WIP technique only heats the samples to 200 °C to remove the formation fluid, there is a possibility that some heavy hydrocarbons are not completely removed and therefore introduce an error in the analysis. Another limitation of this technique is its application in mixed wettability rocks. Deionized water saturates most of the hydrophilic pores but high capillary pressure prevents water intrusion into extremely hydrophobic pores (unless through a forced imbibition process). The deionized water may also cause swelling of some clay minerals which results in overestimation of porosity using this technique [12,39].

While total porosity represents total voidage in the rock, it does not provide information about fluid flow and hydrocarbon storage in the pore system. Quantifying pore structure and mineral surface properties (i.e. pore size distribution, specific surface area, surface charges and cation exchange capacity) helps us in characterizing petrophysical properties of the rock. Different techniques are available for quantifying pore size distribution and specific surface area, for example, mercury intrusion porosimetry (MIP) [17], NMR analysis [40], NMR cryoporometry [41], thermoporometry [42,43] and gas adsorption [10,44–47].

Table 1
Physical properties of organic solvents used for solvent extraction.

Solvent properties	Toluene	Chloroform	MAC[a]	NMP
Boiling point (°C)	110.6	61	57.5	202
Solubility in water (25 °C%w/w)	0.052	0.82	–	Total
Polarity (water 100)	9.9	25.9	36.1	36

[a] MAC: 23 wt% methanol, 30 wt% acetone, 47 wt% chloroform.

Despite wide usage of MIP in conventional reservoir rocks and its ability in capturing a wide range of pores, it is limited to measuring pores with pore throat sizes larger than 3.6 nm. Gas adsorption technique on the other hand, is capable of characterizing pore size distribution in the pores 2–200 nm in diameter. MIP and sub critical gas adsorption techniques have been used as complimentary methods for characterizing a broader range of pore sizes in mudrocks [17,36]. Except when GRI technique is used, all these studies have assumed that pores are accessible to the measuring fluid. However, if some pores are occupied by hydrocarbons, porosity and PSD will be dependent on their pretreatment for hydrocarbon removals.

2.3. Samples and solvent extraction

We studied pore size distribution, specific surface area and geochemical properties of ten Bakken Shale samples after successive solvent extraction. The selection was made from a range of mineralogy and thermal maturity. Table 1 summarizes the physical properties of solvents used. Utilizing a range of solvents with varying polarity and chemical structure enabled us to target a wider range of organic compounds in a successive process, determining the effect of each solvent and to ultimately access larger portions of the pore system.

Aliquots were crushed and sieved with 100 meshes (149 μm). All aliquots were extracted with toluene and then with chloroform in a soxhlet extraction unit for 48 h each. Five samples were further extracted using two solvents with higher polarities. First with a mixture of methanol, acetone and chloroform (MAC) and then with N-methyl-2-pyrrolidone (NMP). Geochemical analysis was performed before extraction on all aliquots and after each extraction on the samples that were only extracted with toluene and chloroform. 2–3 g of aliquots were separated for PSD, SSA and geochemical analysis after each extraction step. LECO TOC method was used for determining organic content and RockEval II for geochemical characterization of the organic matter. It is worthwhile mentioning that there are errors associated with using HI from RockEval as a measure of maturity since these shale samples may not have had the same initial HI. Table 2 summarizes the properties of the samples before and after solvent extraction with toluene and chloroform. Since mostly micropores were expected to be recovered after extraction, subcritical nitrogen adsorption technique was used for PSD and SSA determination as suggested by Kuila et al. [12]. The aliquots were degassed at 120 °C under vacuum (10 μm Hg) prior to performing nitrogen adsorption tests.

Three Bakken Shale samples were used for petrographical analysis. Samples were selected from eastern part of the Williston basin at immature state, central part of the basin at peak

Table 2
Mineralogy, organic matter geochemical properties and pore characteristics of investigated samples before and after successive solvent extraction are shown in the order of decreasing maturity. Silicates: quartz + feldspars, carbs: calcite + dolomite.

Sample	Mineral composition						Before extraction		After toluene extraction		After chloroform extraction		After MAC extraction		After NMP extraction	
	Clays (wt%)	Silicates (wt%)	Carbs (wt%)	Pyrite (wt%)	TOC (wt%)	HI (mg HC/g TOC)	SSA (m^2/g)	Porosity (%)	SSA (m^2/g)	Porosity (%)	SSA (m^2/g)	Porosity (%)	SSA (m^2/g)	Porosity (%)	SSA (m^2/g)	Porosity (%)
EPU 119	25	62	10	3	12.5	6	28.8	6.3	–	–	–	–	–	–	–	–
10694	37	55	6	2	15.5	102	16.2	5.2	51.7	7.8	49.1	7.6	–	–	–	–
10792	28	50	17	5	7.9	126	3.8	2.3	19.9	2.6	30	3.9	28.43	3.1	8.19	1.0
11005	31	57	9	3	12.4	131	17.3	5.1	45.9	15.0	48.8	14.7	–	–	–	–
10479	37	48	10	5	10.3	234	0.8	1.3	0.9	1.3	1.04	1.3	1.37	1.3	0.5	0.8
9157	34	59	3	4	21.7	257	3	2.9	53	6.9	52.8	6.7	–	–	–	–
10368	28	51	16	5	12.8	371	1	1.5	1	1.2	1.6	1.9	1.63	1.7	0.93	1.0
7219	30	65	2	3	16.1	556	1.3	4.1	8.3	4.6	5.7	4.1	–	–	–	–
7216	43	46	5	6	17.7	633	2.6	2.1	3	2.3	5.6	3.7	7.29	4.1	5.07	5.3
7221	37	55	4	4	16	636	1.9	2.1	2.9	2.8	3.6	3.4	8.86	6.7	2.89	3.0

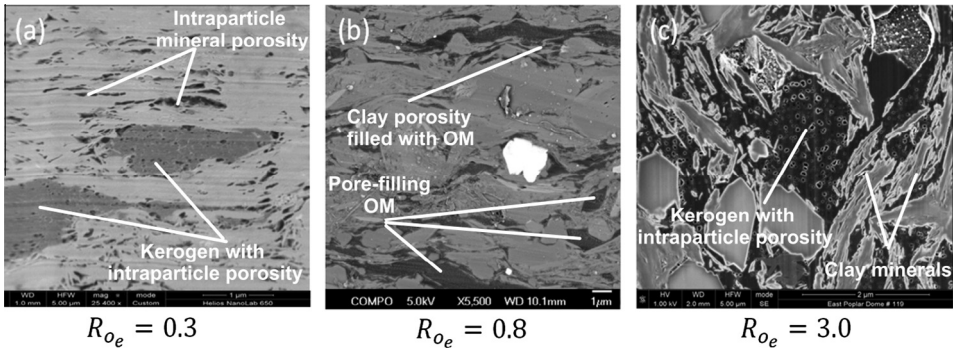

Fig. 1. FIB-SEM images of Bakken Shale samples from different parts of Williston basin with a range of maturity from (a) immature (b) onset oil generation (sample 7221) and (c) dry gas window (sample EPU 119). Equivalent vitrinite reflectance of each sample is denoted by R_{oe}. Higher vitrinite reflectance indicates higher thermal maturity.

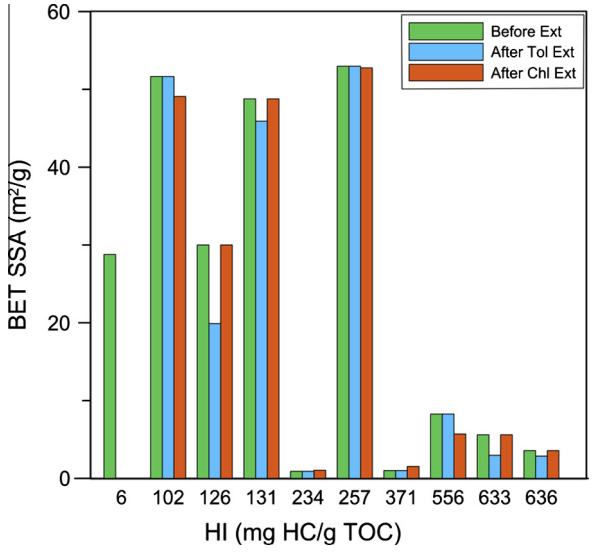

Fig. 2. Specific surface area of the investigated samples before and after solvent extraction. The samples are identified by their maturity index (HI). Lower HI indicates higher maturity.

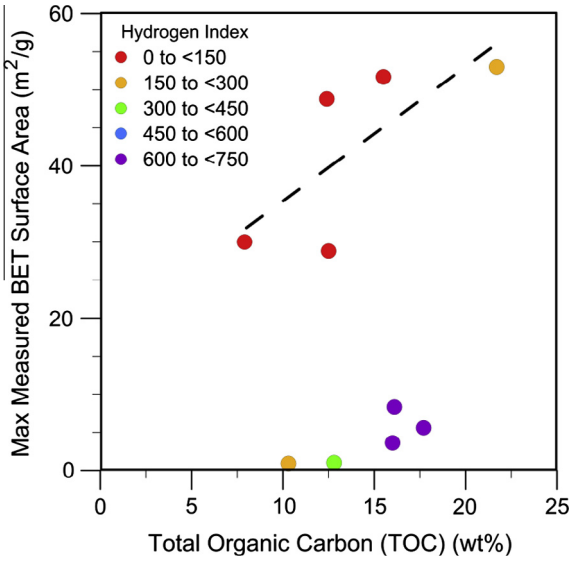

Fig. 3. Maximum measured specific surface area of the aliquots are plotted versus TOC. The gray scale indicates thermal maturity index (HI).

oil generation and western part of the basin at over-mature (gas window) state where the interval is above a laccolith.

3. Results

3.1. Image analysis

Petrographical analysis of Bakken Shale shows a dramatic alteration in the nature of pores and pore-hosting particles with maturity. At immature state (Fig. 1a), two dominant types of pore systems were identified: intraparticle kerogen porosity and interparticle clay porosity. At mature state (Fig. 1b), interparticle porosity is rare; the majority of clay porosity is filled with organic matter while organic matter shows no visible intraparticle porosity. At gas window (Fig. 1c), the predominant pore type is intraparticle organic porosity.

Our observation confirms previous studies that had shown none to very low measurable or visible porosity in the Bakken Shale at oil window [48]. It is of great interest to understand the extent and controlling factors of storage in the source rocks in the oil window. Despite high resolution of available SEM imaging techniques (4–7 nm), a considerable part of the pore space may remain unresolved and it is impossible to distinguish between converted organic matter (bitumen) and kerogen. Therefore, it is not feasible

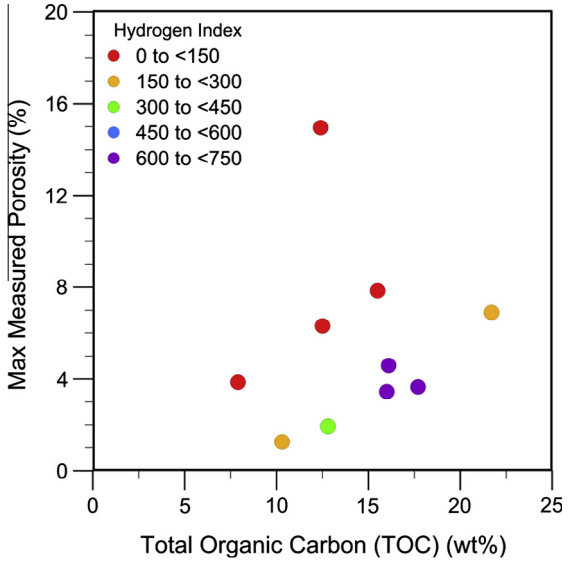

Fig. 4. Maximum measured porosity are plotted versus TOC. The gray scale indicates thermal maturity index (HI). The porosity increases with TOC and more mature samples have relatively higher porosity.

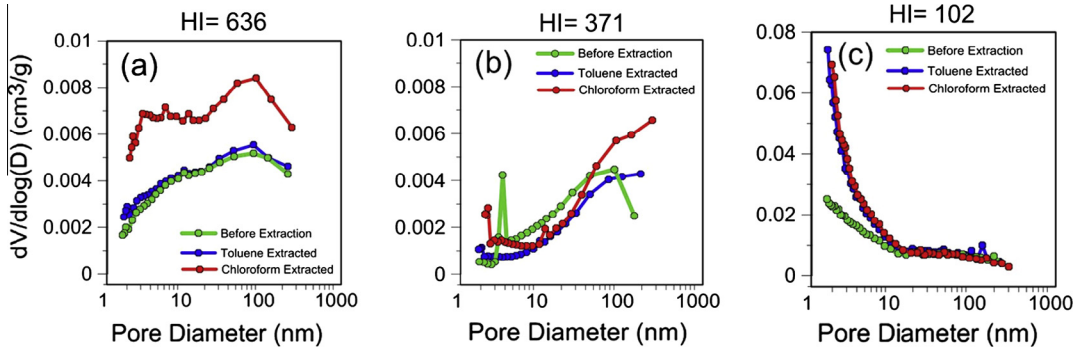

Fig. 5. Example pore size distribution curves of three samples before and after solvent extraction.

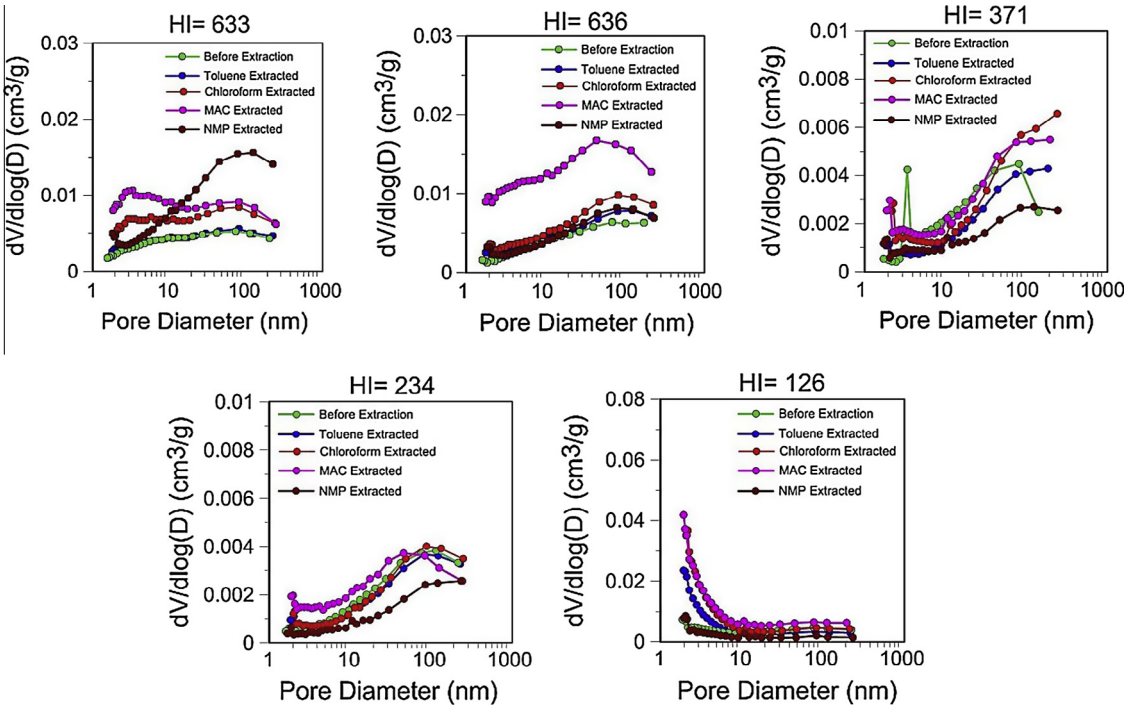

Fig. 6. Pore size distribution of five samples after extraction with Toluene, Chloroform, MAC and NMP in comparison with native state.

to quantify the pore space that is preserved in the oil window but saturated with the bitumen using SEM imaging. However, presence of intraparticle porosity in the kerogen and interparticle porosity in clay minerals at immature state and in the gas window questions vanishing of porosity in the oil window. To quantify this amount, we utilized solvent extraction to remove the bitumen from the pore space and sub-critical nitrogen adsorption for pore characterization.

3.2. Pore characterization

Solvent extraction using toluene and chloroform resulted in significant recovery of the pore space in mature Bakken Shales samples (HI < 300). Both the specific surface area (SSA) and porosity increased after solvent extraction. In some cases specific surface area (SSA) increased from 3 to upwards of 53 m^2/g and porosity increased from 5.1% to 15% (Table 2).

SSA after solvent extraction with toluene and chloroform are compared with native state in Fig. 2. The light gray bars in this figure represents the SSA of each sample before extraction, dark gray bars show SSA after toluene extraction and black bars show SSA after chloroform extraction. Higher initial and recovered surface areas are generally observed in the samples with HI of lower than 300 (mg HC/g TOC) except the sample 10479 (HI = 234 in Fig. 2). As mentioned before the current HI of the samples is not only a function of maximum temperature they have experienced during the geological time, but also a function of initial kerogen types and their fractions. Therefore, current HI might not be a perfect indicator to compare the maturity levels for example between sample 10479 and other samples in the same range of maturity.

The maximum recovered SSA and porosity, after solvent extraction for the samples from oil window and without extraction for the sample from gas window, are plotted versus TOC respectively in Figs. 3 and 4. Mature samples show higher SSA and porosity. The highest maturity sample did not show noticeable change in solvent color and so the PSD and SSA were assumed to not have changed. Porosity and SSA are correlated with TOC.

Comparing pore size distribution (PSD) curves (Fig. 5), shows that in less mature samples the pore size distribution does not change after toluene extraction whereas in more mature samples most of the change occurred after toluene extraction, subsequent chloroform extraction recovered very little additional pore space.

Table 3
Geochemical analysis of organic matter before and after solvent extraction.

Sample	Mineral composition				Before extraction		After toluene extraction		After chloroform extraction	
	Clays (wt%)	Silicates (wt%)	Carbs (wt%)	Pyrite (wt%)	TOC (wt%)	HI (mgHC/gTOC)	TOC (wt%)	HI (mgHC/gTOC)	TOC (wt%)	HI (mgHC/gTOC)
10694	37	55	6	2	15.5	102	14	88	12.4	97
11005	31	57	9	3	12.4	131	12.2	100	11.3	108
9157	34	59	3	4	21.7	257	24.4	226	20.6	266
7219	30	65	2	3	16.1	556	14.2	492	12.9	550
9852	37	55	5	3	19.1	581	18.8	588	25.8	420

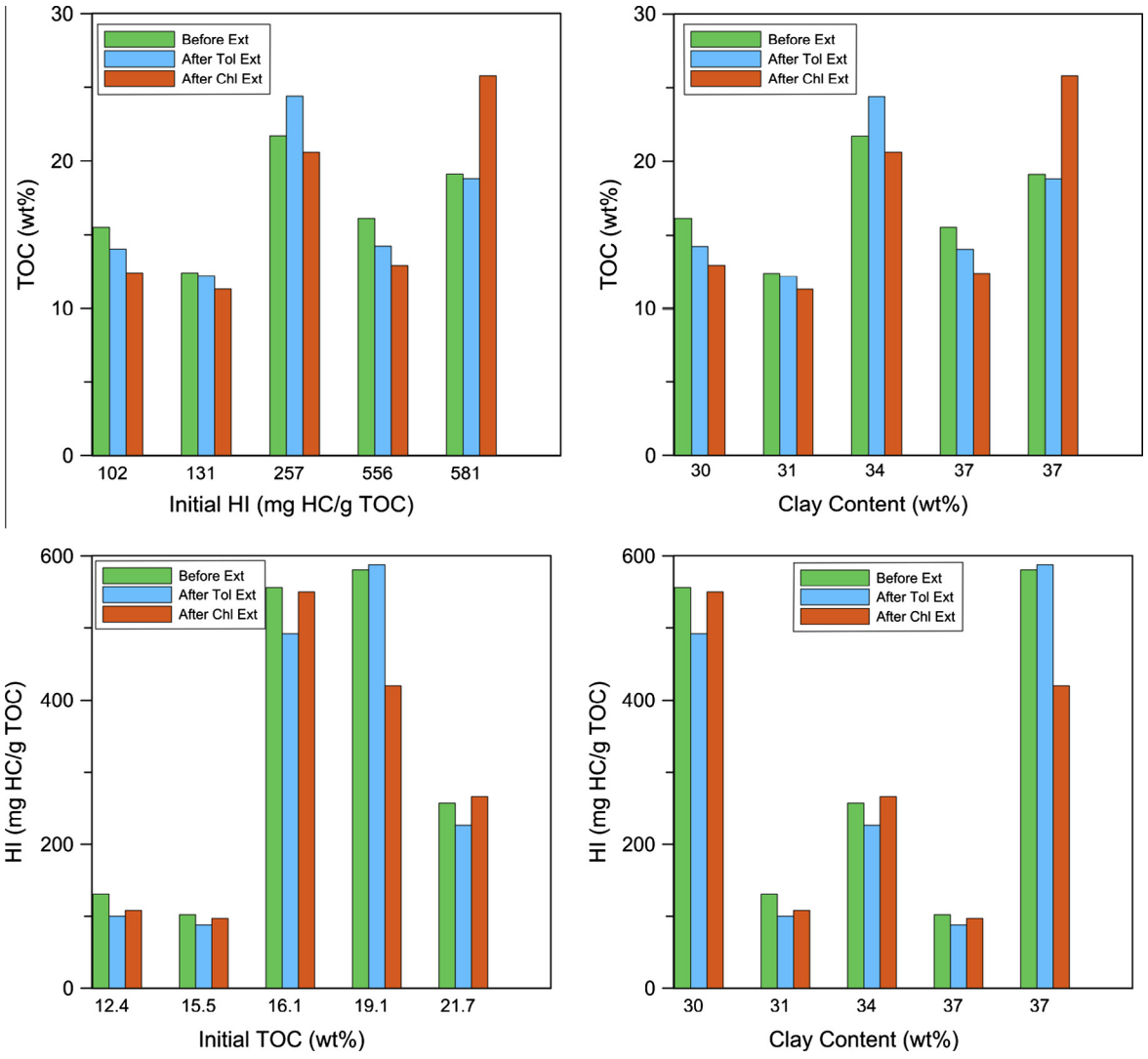

Fig. 7. Change of measured TOC and HI after solvent extraction as a function of clay content, initial TOC and initial HI. There is no significant trend in changes of measured geochemical parameters due to solvent extraction.

Pore size distribution curves for different maturity rocks also vary in shape. The dominant pores in higher maturity samples are mainly smaller than 10 nm (Figs. 5 and 6), whereas in less mature samples larger pores are often dominant.

The question that remains unresolved is why the SSA is so low at the early stages of oil generation despite abundance of intra-particle kerogen and interparticle mineral porosity at immature state. This phenomenon might be due to limited solubility of the heavy bitumen in the solvents used here. In order to further investigate existence of micro pores in less mature states, the successive extraction was continued with MAC and NMP on five samples. SSA and PSD were measured consequently after each extraction (Fig. 6).

Additional recovery of pore space was observed in immature samples after MAC extraction while more mature samples show minimum change in PSD curve after MAC extraction. Effect of NMP on PSD was rather destructive except on larger pores of one of the immature samples (#7216, HI = 633 in Fig. 6).

3.3. Geochemical analysis

RockEval analysis was conducted on five samples after solvent extraction. Total organic content (measured using LECO TOC) and maturity index (hydrogen index) are compared with natural state (Table 3). In general, the results show no evident trend relatable

to initial values of TOC, HI or mineralogy (Fig. 7). The changes in the TOC and HI are, for the most part, within expected errors of these measurements.

4. Discussion

Successive solvent extraction of source rocks revealed abundance of otherwise undetected porosity at the oil window. Mature samples showed higher SSA and porosity which increases with TOC [51]. This is an indication of dominance of kerogen hosted porosity in mature samples, consistent with findings of Kuila et al. [12]. At early stages of maturation, chemical decomposition of kerogen is found to produce insoluble organic compound and become rubber-like [49,50]. Both mechanisms may cause collapsing or filling of the kerogen hosted pores at the oil window [12].

At higher maturity levels, most of the soluble pore-filling hydrocarbon can be extracted using toluene. However, at lower maturity the bitumen can be more efficiently dissolved using more polar solvents. This phenomenon suggests a possible difference in composition of the bitumen and/or its interaction with the pore-hosting grains.

While chloroform and MAC improved the extraction of bitumen, NMP resulted in porosity reduction. Similar effect was observed when different clay minerals (i.e. illite, smectite and kaolinite) were exposed to NMP [52]. This behavior in organic rich shales is due to swelling of kerogen (and maybe clays) as found by Hruljova et al. [53]. It could also be partly due to mobilizing and transporting the bitumen by NMP from larger pores to smaller (potentially more oil wet) pores.

An increase in TOC or HI after solvent extraction was unexpected since some fraction of organic matter was removed from the source rock. This can only be explained by absorbing of utilized solvent in organic matter and/or adsorbing on the clay surfaces.

Presence of kerogen-hosted porosity affects petrophysical, mechanical and flow properties of the source rocks. Porous kerogen has lower stiffness modulus [7] which causes softening the rock matrix frame especially if kerogen is load bearing. Kerogen porosity contributes in hydrocarbon storage in the source rocks, however its significance in contributing to flow will depend on the overall pore system morphology.

5. Conclusions

Source rocks contain considerable porosity in the oil window which is often entirely or partially filled with bitumen. Porosity and pore morphology measurements using available techniques can be affected by occupancy of the pores by the bitumen. Solvent extraction enables us to access the pore space in order to produce a more complete image of the pore system in the mudrocks. Utilizing organic solvents increases accessibility to the pore system in organic rich rocks at the oil window, however very high polarity solvents (i.e. NMP) showed a destructive effect on pore morphology. Based on the results with various solvents on the Bakken Shale, NMP is not recommended as a routine cleaning solvent for pore characterization purposes because of the potential swelling effect on kerogen.

Our SSA and PSD data confirms that there is an overwhelming population of kerogen hosted porosity in the nanometer-scale range (<10 nm) at the oil window. We found that the kerogen porosity generation peaks at higher maturity samples with HI of less than 300 (mg HC/g TOC). The total porosity and surface area was also found to be directly related to TOC in the higher maturity samples.

We found no particular effect of rock mineralogy, especially clay content, on the porosity development in organic rich shales.

Acknowledgements

We would like to thank members of OCLASSH consortium at Colorado School of Mines for financially supporting this project, Whiting Petroleum Corporation for providing us with samples, Dr. Douglas McCarty at Chevron ETC for performing XRD analysis, Ilaria Erico, Marina Lordello, Lemuel Godinez and Anrei Panfilau for their help in PSD, SSA and solvent extraction experiments. Dr. Stuti Gaur helped us with solvent selection. SEM images were acquired at the Whiting Rock Lab in Denver, Colorado.

References

[1] Katsube TJ, Scromeda N. Effective porosity measuring procedure for low porosity rocks. Geol Surv Can 1991:291–7 [91-1E].
[2] Howard JJ. Porosimetry measurement of shale fabric and its relationship to illite/smectite diagenesis. Clays Clay Miner 1991;39:355–61.
[3] Dorsch J, Katsube TJ. Effective porosity and pore-throat sizes of mudrock saprolite from the Nolichucky shale within Bear Creek Valley on the Oak Ridge Reservation: implications for contaminant transport and retardation through matrix diffusion. Technical Report Oak Ridge National Lab., Environmental Sciences Division, TN, USA; 1996 [No. ORNL/GWPO-025].
[4] Kurtoglu B. integrated reservoir characterization and modeling in support of enhanced oil recovery for Bakken. PhD thesis: Colorado School of Mines; 2013.
[5] Okiongbo S, Aplin AC, Larter SR. Changes in type II kerogen density as a function of maturity: evidence from the Kimmeridge clay formation. Energy Fuel 2005;19(6):2495–9.
[6] Prasad M, Mba K, McEvoy TE, Batzle ML. Maturity and impedance analysis of organic-rich shales. SPE Reserv Eval Eng 2011;14(5):533–43.
[7] Zargari S, Prasad M, Mba KC, Mattson ED. Organic maturity, elastic properties, and textural characteristics of self resourcing reservoirs. Geophysics 2013;78(4):223–35.
[8] Wilkinson TM, Zargari S, Prasad M, Packard CE. Optimizing nano-dynamic mechanical analysis for high-resolution, elastic modulus mapping in organic-rich shales. J Mater Sci 2014:1–9.
[9] Loucks RG, Reed RM, Ruppel SC, Hammes U. Spectrum of pore types and networks in mudrocks and a descriptive classification for matrix-related mudrock pores. AAPG Bull 2012;96:1071–98.
[10] Kuila U, Prasad M. Specific surface area and pore-size distribution in clays and shales. Geophys Prospect 2013;61(2):341–62.
[11] Larsen JW, Kidena K. The sudden release of oil and bitumen from Bakken Shale on heating in water. Energy Fuel 2002;16(4):1004–5.
[12] Kuila U, McCarty DK, Derkowski A, Fischer TB, Topór T, Prasad M. Nano-scale texture and porosity of organic matter and clay minerals in organic-rich mudrocks. Fuel 2014;135:359–73.
[13] Bohacs KM, Passey QR, Rudnicki M, Esch WL, Lazar OR. The spectrum of fine-grained reservoirs from 'shale gas' to 'shale oil'/tight liquids: essential attributes, key controls, practical characterization. In: International petroleum technology conference, Beijing, China; 2013 [IPTC 16676].
[14] Lewan MD, Birdwell JE. Application of uniaxial confining-core clamp with hydrous pyrolysis in petrophysical and geochemical studies of source rocks at various thermal maturities. unconventional resources technology conference (URTeC), Denver; 2013 [SPE 168691].
[15] Javadpour F, Fisher D, Unsworth M. Nanoscale gas flow in shale gas sediments. J Can Pet Technol 2007;46(10):55–61.
[16] Javadpour F. Nanopores and apparent permeability of gas flow in mudrocks (shales and siltstone). J Can Pet Technol 2009;48(8):16–21.
[17] Ross DJK, Bustin RM. The importance of shale composition and pore structure upon gas storage potential of shale gas reservoirs. Mar Pet Geol 2009;26(6):916–27.
[18] Zhang T, Ellis GS, Ruppel SC, Milliken K, Yang R. Effect of organic-matter type and thermal maturity on methane adsorption in shale-gas systems. Org Geochem 2012;47:120–31.
[19] Lagaly G. Clay-organic interactions. Philos Trans Royal Soc Lond. A Math Phys Sci 1984;311(1517):315–32.
[20] Kowalska M, Güler H, Cocke DL. Interactions of clay minerals with organic pollutants. Sci Total Environ 1994;141(1):223–40.
[21] Theng BKG. Interactions of clay minerals with organic polymers: some practical applications. Clays Clay Miner 1970;18:357–62.
[22] Theng BKG. The chemistry of clay-organic reactions. London: Adam-Hilger; 1974.
[23] Warren DS, Clark AI, Perry R. A review of clay-aromatic interactions with a view to their use in hazardous waste disposal. Sci Total Environ 1986;54:157–72.
[24] Bernard S, Wirth R, Schreiber A, Schulz H-M, Horsfield B, Hors B. Formation of nanoporous pyrobitumen residues during maturation of the Barnett Shale (Fort Worth Basin). Int J Coal Geol 2012;103:3–11.

[25] Curtis ME, Cardott BJ, Sondergeld CH, Rai CS. The development of organic porosity in the Woodford shale as a function of thermal maturity. SPE annual technical conference and exhibition, San Antonio, Texas, USA; 2012 [SPE 160158].
[26] Modica CJ, Lapierre SG. Estimation of kerogen porosity in source rocks as a function of thermal transformation: example from the Mowry Shale in the Powder River Basin of Wyoming. AAPG Bull 2012;96:87–108.
[27] Lordello MC, Erico I, Zargari S, Prasad M. Variations in pore size distributions in organic matter and clay minerals from dissolution studies. In: The Goldschmidt conference, Sacramento, California, USA; 2014.
[28] Wei L, Mastalerz M, Schimmelmann A. Thermal evolution of porosity in organic-rich shales: The influence of Soxhlet-extractable bitumen/oil. In: The Goldschmidt conference, Sacramento, California, USA; 2014.
[29] Wei L, Mastalerz M, Schimmelmann A, Chen Y. Influence of Soxhlet-extractable bitumen and oil on porosity in thermally maturing organic-rich shales. Int J Coal Geol 2014;132:38–50.
[30] Saidian M, Rasmussen T, Nasser M, Mantilla A, Tobin R. Qualitative and quantitative reservoir bitumen characterization: a core to log correlation methodology. Interpretation 2015;3(1):SA143–58.
[31] Loucks RG, Reed RM, Ruppel SC, Jarvie DM. Morphology, genesis, and distribution of nanometer-scale pores in siliceous mudstones of the Mississippian Barnett Shale. J Sediment Res 2009;79:848–61.
[32] Loucks RG, Reed RM, Ruppel SC, Hammes U. Preliminary classification of matrix pores in mudrocks. Gulf Coast Assoc Geol Soc Trans 2010;60:435–41.
[33] Curtis ME, Ambrose RJ, Sondergeld CH, Rai CS. Structural characterization of gas shales on the micro- and nano-scales. In: Canadian unconventional resources and international petroleum conference, Calgary, Alberta, Canada; 2010 [SPE 137693].
[34] Diaz E, Sisk C, Nur A. Quantifying and linking shale properties at a variable scale, presented at 44th U.S. rock mechanics symposium and 5th U.S. – Canada rock mechanics symposium, Salt Lake City, Utah, USA; 2010 [ARMA 10-272].
[35] Slatt RM, O'Brien NR. Pore types in the Barnett and Woodford gas shales: contribution to understanding gas storage and migration pathways in fine-grained rocks. AAPG Bull 2011;95(12):2017–30.
[36] Saidian M, Kuila U, Godinez LJ, Rivera S, Prasad M. Porosity and pore size distribution in mudrocks: a comparative study for Haynesville, Niobrara, Monterey, and Eastern European Silurian Formations. Unconventional Resources Technology Conference (URTEC), Denver, Colorado, USA; 2014b.
[37] Luffel DL, Guidry FK, Curtis JB. Evaluation of Devonian shale with new core and log analysis methods. J Petrol Technol 1992;44(11):1–192.
[38] Kuila U, McCarty DK, Derkowski A, Fischer TB, Prasad M. Total porosity measurement in gas shales by the water immersion porosimetry (WIP) method. Fuel 2014;117:1115–29.
[39] Saidian M, Kuila U, Godinez LJ, Rivera S, Prasad M. A Comparative Study of Porosity Measurement in Mudrocks. Denver (Colorado, USA): SEG Annual Meeting; 2014.
[40] Latour LL, Mitra PP, Kleinberg RL, Sotak CH. Time-dependent diffusion coefficient of fluids in porous media as a probe of surface-to-volume ratio. J Magn Reson, Ser A 1993;101(3):342–6.
[41] Strange JH, Rahman M, Smith EG. Characterization of porous solids by NMR. Phys Rev Lett 1993;71(21):3589–91.
[42] Ishikiriyama K, Todoki M, Min KH, Yonemori S, Noshiro M. Thermoporosimetry: pore size distribution measurements for microporous glass using differential scanning calorimetry. J Therm Anal 1996;46:1177–89.
[43] Brun M, Lallemand A, Quinson JF, Eyraud C. A new method for the simultaneous determination of the size and shape of pores: the thermoporometry. Thermochim Acta 1977;21(1):59–88.
[44] Adesida A. Pore size distribution of Barnett Shale using nitrogen adsorption data, MSc thesis: University of Oklahoma; 2011.
[45] Chalmers GR, Bustin RM, Power IM. Characterization of gas shale pore systems by porosimetry, pycnometry, surface area, and field emission scanning electron microscopy/transmission electron microscopy image analyses: examples from the Barnett, Woodford, Haynesville, Marcellus, and Doig units. AAPG Bull 2012;96:1099–119.
[46] Clarkson C, Freeman M, He L, Agamalian M, Melnichenko Y, Mastalerz M, et al. Characterization of tight gas reservoir pore structure using USANS/SANS and gas adsorption analysis. Fuel 2012;95:371–85.
[47] Clarkson C, Wood J, Burgis S, Aquino S, Freeman M. Nanopore-structure analysis and permeability predictions for a tight gas siltstone reservoir by use of low pressure adsorption and mercury-intrusion techniques. SPE Reserv Eval Eng 2012;15:648–61.
[48] Vernik L, Liu X. Velocity anisotropy in shales: a petrophysical study. Geophysics 1997;62(2):521–32.
[49] Johnson WF, Walton DK, Keller HH, Couch EJ. In situ retorting of oil shale rubble: a model of heat transfer and product formation in oil shale particles. Quarterly of the Colorado School of Mines, USA; 1975, 70:3.
[50] Schnackenberg WD, Prien CH. Effect of solvent properties in thermal decomposition of oil shale Kerogen. Ind Eng Chem 1953;45:313–22.
[51] Passey QR, Bohacs KM, Esch WL, Klimentidis R, Sinha S. From oil-prone source rock to gas-producing shale reservoir–geologic and petrophysical characterization of unconventional shale-gas reservoirs. In: International oil and gas conference and exhibition, Beijing, China; 2010.
[52] Erico I. Oil shale samples characterization for reservoir evaluation. MSc thesis: Polytechnic University of Turin; 2014.
[53] Hruljova J, Savest N, Oja V, Suuberg EM. Kukersite oil shale kerogen solvent swelling in binary mixtures. Fuel 2013;105:77–82.